Thermochimica Acta 517 (2011) 81–89

Contents lists available at ScienceDirect

Thermochimica Acta

journal homepage: www.elsevier.com/locate/tca

Non-isothermal kinetic analysis of the devolatilization of corn cobs and sugar cane bagasse in an inert atmosphere

Akinwale O. Aboyade[a,b], Thomas J. Hugo[a], Marion Carrier[a], Edson L. Meyer[b], Ralph Stahl[c], Johannes H. Knoetze[a], Johann F. Görgens[a,*]

[a] Department of Process Engineering, Stellenbosch University, Stellenbosch, South Africa
[b] Fort Hare Institute of Technology, University of Fort Hare, Alice, South Africa
[c] Institute of Technical Chemistry-Division of Chemical and Physical Processing, Forschungszentrum Karlsruhe, Germany

ARTICLE INFO

Article history:
Received 10 August 2010
Received in revised form 21 January 2011
Accepted 26 January 2011
Available online 5 March 2011

Keywords:
Biomass
Devolatilization
Pyrolysis
Thermogravimetric analysis (TGA)
Non-isothermal
Kinetic analysis
Corn cobs
Sugar cane bagasse

ABSTRACT

Corn cobs and sugar cane bagasse are two of the most important agricultural residues in South Africa in terms of availability and potential for use as a bioenergy resource. The thermal devolatilization of samples of these two fuels in an inert atmosphere was studied by non-isothermal thermogravimetric analysis in the heating rate range of 10–50 °C min^{-1}. Friedman's isoconversional method was applied using the AKTS Thermokinetics software to obtain the dependence of activation energy on conversion. The same method was also applied to the kinetic analysis of lignocellulosic pseudocomponents derived from the mathematical deconvolution of the original DTG curves. The results showed that apparent activation energy in the 0.1–0.8 conversion interval ranged from 170–225 kJ mol^{-1} to 75–130 kJ mol^{-1} for sugar cane bagasse and corn cobs respectively. The range of apparent activation energy obtained for the pseudocomponents representing hemicelluloses, cellulose and lignin derived from sugar cane bagasse were given as 200–300 kJ mol^{-1}, 163–245 kJ mol^{-1}, and 80–180 kJ mol^{-1}, while for corn cobs the values were 85–110 kJ mol^{-1}, 80–140 kJ mol^{-1}, and 10–60 kJ mol^{-1} respectively. The derived thermokinetic parameters from both global and pseudocomponent analyses satisfactorily reproduced the experimental curves used for the analysis and could also successfully predict reaction progress at a heating rate outside what was used in the analysis. The fits obtained between simulated and experimental results were comparable to what has been reported in the literature based on conventional model-fitting techniques.

1. Introduction

Various procedures for evaluating kinetic parameters from data derived from non-isothermal thermogravimetric analysis (TGA) have been developed, and the vast majority of them can be classified as either 'model-free' or 'model-fitting'. Until recently, the model-fitting approach has found wider application in biomass thermochemical conversion studies, although it is widely recognised that the method suffers from two main deficiencies, particularly in cases where data from only a single heating rate is applied: i) it can often yield different values of kinetic parameters describing the same thermogravimetric curve, leading to an ambiguity in terms of interpretation of the results; ii) it generally tends to yield one set of kinetic parameters for the whole range of conversion, therefore not taking into account the complexity of mechanisms involved during pyrolysis of plant biomasses. Applying model fitting to datasets from multiple heating rates addresses the first concern [1] but not the second [2]. On the other hand, model-free methods shown to be effective in overcoming the aforementioned problems associated with model fitting [2–4]. As the name implies, model-free techniques do not require assumption of reaction models, and yield kinetic parameters as a function of either conversion (isoconversional analysis) or temperature (non-parametric kinetics) [3].

The isoconversional approach is the more commonly adopted of the two main model-free methods and is increasingly being adopted in biomass thermochemical conversion research. In 2001, Garcià-Pèrez et al. [5] employed Friedman's isoconversional approach to the study of the pyrolysis kinetics of sugar cane bagasse. More recently, Biagini et al. [6,7], Cai et al. [8–10], Leroy et al. [11], Gašparovič et al. [12], Xiao et al. [13], Tonbul [14], and Santos et al. [15], have all employed various isoconversional methods in the analysis of the non-isothermal decomposition of biomass and/or its components. Only a few of these studies [11,12] attempted to validate their model-free derived kinetic parameters by simulating or predicting the non-isothermal experimental data. According to Varhegyi [1] the lack of comparison of analytical results with experimen-

* Corresponding author. Tel.: +27 21 808 3503; fax: +27 21 808 2059.
E-mail address: jgorgens@sun.ac.za (J.F. Görgens).

0040-6031/$ – see front matter © 2011 Elsevier B.V. All rights reserved.
doi:10.1016/j.tca.2011.01.035

Table 1
Proximate and ultimate characteristics of corn cobs (CC) and sugar cane bagasse (SB) from this study and from other authors.

	CC Present study	SB Present study	CC Ioannidou et al. [30]	CC Sonobe et al. [49]	SB Drummond and Drummond [43]	SB Munir et al. [45]
Proximate analysis (wt.% dry basis)						
Moisture	6.5	6.8	7.6			
Volatiles	80.2	76.9	84.3	82.2	86.5	81.5
Fixed Carbon[a]	16.7	17.8	7.63	16.9	11.9	13.3
Ash	3.1	5.3	8.06	0.9	1.6	5.2
HHV (MJ/kg)	17.2	17.5	18.3 (LHV)			17.7
Ultimate analysis (wt.% dry and ash free basis)						
C	49.0	50.3	43.8	45.5	46.3	46.2
H	6.0	6.3	6.2	6.2	6.3	6.3
O[a]	44.7	43.1	50	37.9	47.2	45.7
N	0.3	0.3		1.3	0.2	1.8
S	0.08	0.07		0.0		

[a] Calculated by difference.

tal data calls into question the reliability of derived kinetic parameters.

The present work aims at obtaining information on the devolatilization behaviour and kinetics of corn cobs and sugar cane bagasse. These two feedstocks represent the bulk of agricultural residue in South Africa that is potentially available for bioenergy production [16,17]. It has been estimated that up to 3.3 and 6.7 million tonnes of sugar cane bagasse and corn residue are generated in South Africa per annum, representing an energy equivalence of 118 and 58 PJ/yr, respectively [16]. Friedman's isoconversional method has been employed to obtain the variation of kinetic parameters over the entire range of conversion for the samples. Furthermore, a unique approach was employed to derive kinetic parameters of the constituent lignocellulosic pseudocomponents. Global TGA data of the samples were deconvoluted and the separated peaks representing hemicelluloses, cellulose and lignin were subjected to the same Friedman's analysis. Predictions based on the derived kinetic parameters were compared with experimental data in order to obtain an indication of the reliability of the kinetic approach employed.

2. Material and methods

2.1. Samples

Dried corn cobs (CC) were collected from a farm in the Free State province in South Africa, soon after grain harvesting in 2008. Sugar cane bagasse (SB) used in this work was provided by the South African Sugar Milling Research Institute (SMRI). First, dried samples of both materials were chopped to a particle size <1 mm; afterwards representative fractions were milled using a cryogenic grinder and sieved with a fraction of 125–350 μm retained for the experimental runs. The proximate and ultimate characteristics of CC and SB from this study as well as from previous studies by other authors are presented in Table 1.

2.2. Experimental method

The higher heating value (HHV) of the samples was measured using a plain jacket calorimeter (Parr Instruments, USA, Model 1341). Ultimate analysis was done using a Vario EL elemental analyzer (Elementar Analysensysteme, Hanau, Germany). A Netzsch STA 409 balance was used for thermogravimetric analysis. Low sample masses and particle sizes (approximately 20–50 mg, and <350 μm) were used in order to reduce the occurrence of secondary vapour–solid interactions, and the effects of mass and intra-particle heat transfer [18]. For each experimental run, samples were held at room temperature for 15 min, heated to 105 °C and held again for 30 min. At this stage, the sample mass would have stabilized at a constant dry weight and was then heated to 700 °C at the following heating rates; 10 °C min^{-1}, 20 °C min^{-1}, 30 °C min^{-1}, 40 °C min^{-1}, and 50 °C min^{-1}. These low heating rates are characteristic of fixed bed processes [19,20]. The nitrogen flow during pyrolysis was set to be 55 mL min^{-1} (protective gas into the balance) plus 15 mL min^{-1} directly into the oven chamber. For combustion of the formed char, the temperature was maintained at 700 °C for a further 30 min and the nitrogen flow into the balance was kept constant at 55 mL min^{-1} and 15 mL min^{-1} of oxygen were fed into the oven (instead of 15 mL min^{-1} nitrogen). Variation of the sample residual mass with respect to time and temperature change (TG data), and its derivative with respect to time (DTG data), were continuously collected using the Netzsch Proteus software.

2.3. Kinetic analysis

Kinetic evaluation in this study focuses on the temperature range where devolatilization mainly occurs, i.e. 115–500 °C (corresponding to stages 2 and 3 of Fig. 1). Curves derived from 10–40 °C min^{-1} heating rate experiments were used in the analysis. The kinetic analysis of the thermal decomposition of biomass is usually based on the rate equation for solid state decomposition processes [3,21]

$$\frac{d\alpha}{dt} = A \exp\left[-\frac{E}{RT}\right] f(\alpha) \quad (1)$$

where α is the reacted fraction of the sample or conversion, $f(\alpha)$ is the reaction model, A and E are the Arrhenius—pre-exponential factor and activation energy, respectively. The isoconversional approach does not require the choosing of a reaction model and is thus 'model-free'. It allows the estimation of E as a function of conversion, α independent of the reaction model, $f(\alpha)$. The most common application of the isoconversional analysis was developed by Friedman [22] and is used in this work. The method involves computing the logarithms of the Arrhenius rate equation to get:

$$\ln\left(\frac{d\alpha}{dt}\right) = \ln\left(\beta\frac{d\alpha}{dT}\right) = \ln[A \cdot f(\alpha)] - \frac{E}{RT} \quad (2)$$

A plot of $\ln(d\alpha/dt)_i$ against $1/T_i$ at the same degree of conversion from data taken at various heating rates will result in a series of lines, each with slope equal to $-E/R$ corresponding to each value of conversion, α, at different heating rates β. Thus the dependence of E and $\ln(A{\cdot}f(\alpha))$ on α can be obtained.

A multi-component analysis approach is also frequently adopted as part of the kinetic study of biomass degradation [1,23–25]. In this approach, biomass is generally assumed to be

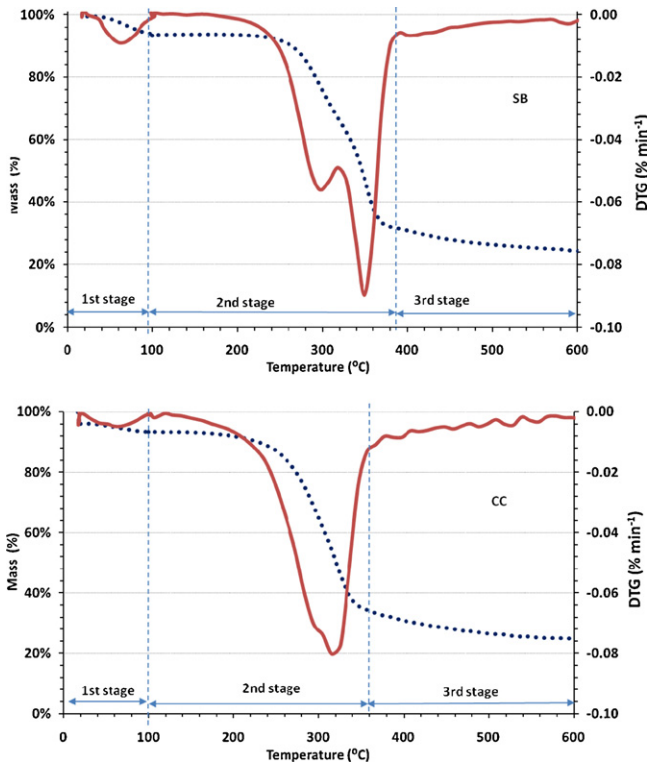

Fig. 1. TG and DTG curves of CC and SB at 10 °C min^{-1} heating rate with TG (●●●) and DTG (▬) curves.

composed of pseudocomponents reacting in parallel or in series [1]. Assuming parallel, multi-component reactions, Eq. (1) becomes;

$$\frac{d\alpha}{dt} = \sum \gamma_i A_i \ \exp\left[-\frac{E_i}{RT}\right] f(\alpha_i) \tag{3}$$

where γ_i is the contribution of pseudocomponent i to the total mass loss, Normally, such multi-component analysis of biomass devolatilization kinetics is conducted via the model-fitting approach [1,23,26]. However, in this study the Friedman's method has been applied to the evaluation of the kinetics of individual pseudocomponents present in the biomass. Global DTG curves for each heating rate considered were first deconvoluted into three peaks corresponding to the pseudocomponents—hemicelluloses, cellulose and lignin. Deconvolution was done based on the application of Gaussian and/or Fraser-Suzuki (asymmetric) type signals [27]. The fitting of calculated signal to the experimental data is performed using Marquardt's non-linear optimization [27].

Simulation of experimental curves was obtained from the following expression [2,4];

$$t_\alpha = \frac{1/\beta \int_0^{T\alpha} \exp(-E_\alpha/RT)dT}{\exp(-E_\alpha/RT_0)} \tag{4}$$

where t refers to the time, R refers to the gas constant, β refers to the heating rate and T_0 refers to initial temperature. The integral in Eq. (4) is solved based on values of E_α and T_α which are obtained directly from tables derived from Eq. (2). The obtained quality of fit (QOF) between simulated and experimental curves was evaluated via the expression:

$$\mathrm{QOF}(\%) = 100 \times \sum_{i=1}^{N_k} \frac{\sqrt{\left\{(d\alpha/dt)_{\mathrm{exp}} - (d\alpha/dt)_{\mathrm{calc}}\right\}^2/N_k}}{\mathrm{Max}\left|d\alpha/dt\right|_{\mathrm{exp}}} \tag{5}$$

where N_k is the number of experimental points employed. The AKTS-Thermokinetics software was used for all kinetic analysis in this study [27]. The software allows the baseline optimization of data curves simultaneously with the estimation of kinetic parameters [27,28].

Table 2
Devolatilization parameters for CC and SB at different heating rates.

Sample	Heating rate (°C min−1)	T_h (°C)	T_c (°C)	T_f (°C)	$\%R_{ash}$ (at 680 °C)
CC					
	10	283	318	330	20.3
	20	305	330	365	20.8
	30	308	337	375	20.0
	40	312	339	387	19.5
SB					
	10	295	350	376	24.1
	20	307	362	391	19.5
	30	312	370	400	18.7
	40	320	374	412	21.6

T_f: the final temperature of cellulose degradation.
T_h, T_c: the peak temperature corresponding to a maximum weight loss for hemicelluloses and cellulose, respectively.
$\%R_{ash}$: the final residue.

3. Results and discussions

3.1. Description of thermoanalytical curves

Fig. 1 shows mass loss (TG) and derivative mass loss (DTG) curves for SB and CC at 10 °C min^{-1} under inert atmosphere. In general, three distinct weight loss stages could be identified, in agreement with previous findings [29–31]. The first stage, corresponding to the reduction in mass at temperatures lower than 100 °C can be attributed to the demoisturization of the samples, 6.5–11.8 wt.% and 5.0–7.1 wt.% respectively for CC and SB. In the second stage, the temperature range 100–200 °C, we see negligible weight loss (<1.5% for CC, and <1% for SB), which was followed by the start of devolatilization characterized by rapid weight loss, at 200 °C for CC and at 230 °C for SB. The insignificant weight loss prior to the start of devolatilization has been attributed to the removal of bound moisture and the start of polysaccharide hydrolysis [29,32].

Lignocellulosic biomasses are comprised of hemicelluloses, cellulose and lignin as the major components [33]. The second stage of weight loss depicted in Fig. 1 corresponds mainly to the degradation of these components [34]. Hemicelluloses typically decompose in the range of 160–360 °C, while cellulose degrades at the higher temperature range of 240–390 °C [23]. The loss of lignin typically occurs at a slower rate over a much wide temperature range of 180–900 °C [18,23,35]. On the DTG curves the temperatures at which maximum rate of weight loss occurred are described by the position of the peaks in the curve. The DTG curve of SB during the devolatilization stage shows two distinct peaks which are represented by a noticeable change in slope of the TG curve. The DTG peaks are much closer to each other for CC than for SB and the maximum of hemicelluloses and cellulose peaks occurring at lower temperatures. Antal and Varhegyi [18] ascribed the cause of the merged DTG peaks to the catalytic behaviour of mineral matter present in biomass, which may explain why SB with an ash content of 5.3% exhibits a more distinct peak compared to CC which has 3.1% ash content.

The third stage, starting from the base of the DTG peak assigned to cellulose (Fig. 1), has a much lower rate of weight loss (12% for CC and 10% for SB) than the second stage (58% for CC and 60% for SB). According to Roque-Diaz et al. [29], for SB, this stage of biomass decomposition corresponds partly to the end of cellulose decomposition, and partly to the beginning of secondary decomposition of heavier volatiles and the formation of char. The decomposition of lignin has also been reported to continue into this stage [31].

Table 2 shows the effect of heating rate on peak temperatures and fraction of mass remaining at the end of conversion. The posi-

Table 3
Relative contributions of pseudocomponents obtained from deconvolution.

Heating rate (°C min^{-1})	γ_i–CC (%)			γ_i–SB(%)		
	Hemicelluloses	Cellulose	Lignin	Hemicelluloses	Cellulose	Lignin
10	54.5	28.4	17.1	20.5	38.3	41.2
20	44.3	39.5	16.2	23.9	48.8	27.3
30	46.7	31.9	21.4	27.1	42.7	30.2
40	52.6	25.9	21.5	25.6	43.1	31.3
Average	49.5	31.4	19.1	24.3	43.2	32.5

tion of peaks ascribed to hemicelluloses and cellulose in SB shifted from 295 °C to 321 °C and from 350 °C to 376 °C respectively. For CC, the peaks in the DTG curve are so close that they tended to overlap, especially at higher heating rates. According to Haykiri-Acma et al. [36] and Di Blasi [37] the overlapping of DTG peaks was probably due to sufficiently low heating rates allowing enough time for each individual component in the biomass to decompose at its own typical peak temperature, while at high heating rates decomposition is almost simultaneous and as such adjacent peaks representing hemicelluloses and cellulose are merged to form broader peaks.

3.2. Global kinetic analysis

Apparent E and $\ln(A{\cdot}f(\alpha))$ values for both SB and CC calculated via Friedman's method are presented in Fig. 2. The plots also show correlation coefficients for the parameter estimation over the entire conversion range. The correlation coefficients relate to the linearity (R^2) of the lines joining isoconversional points on the Friedman's plots, i.e. plots of $\ln(d\alpha/dt)i$ against $1/T_i$ described earlier. It highlights the limitations arising from experimental data variations in the beginning and towards the end of thermogravimetric pyrolytic conversion [6]. For this reason, further discussions will focus on the 0.1–0.9 (0.8 for CC) conversion range.

The overall trend of apparent activation energy (E) dependence on α was relatively similar for both CC and SB in the sense that E more or less increased in the 0.1–0.6 conversion ranges for both materials, followed by a reduction at higher conversion levels. At the start of CC devolatilization, E increased from just less than 100 kJ mol^{-1} to peak at 150 kJ mol^{-1} (at $\alpha = 0.2$). This was followed by a further increase until a new peak of 160 kJ mol^{-1} was reached at about $\alpha = 0.6$. Another peak in the apparent activation energy curve can be observed at about $\alpha = 0.9$ although the low correlation coefficient at this point implies the values might be more unreliable. The apparent E curve for SB was smoother, starting with an initial peak of about 200 kJ mol^{-1} at $\alpha = 0.05$, increasing to the highest point of 225 kJ mol^{-1} at about $\alpha = 0.5$. Thereafter, E decreased reaching 150 kJ mol^{-1} at $\alpha = 0.9$. The range of overall E values obtained here for SB agreed well with those arrived at by Garcià-Pèrez et al. [5] using the same isoconversional method, i.e. 150–200 kJ mol^{-1} in the conversion range, 0.05–0.75. No isoconversional based literature was available to compare CC results with, although Cao et al. [38] and Zabaniotou et al. [39] obtained 68–176 kJ mol^{-1} and 65–75 kJ mol^{-1} respectively, using a curve fitting approach based on single first order reaction model.

The E values presented in the results are not the actual activation energy of any particular single reaction step, but is rather an aggregate (or apparent) value reflecting the contributions of numerous competing and parallel reaction steps to the overall reaction rate. These contributions, for a complex process such as biomass devolatilization, are known to vary with respect to temper-

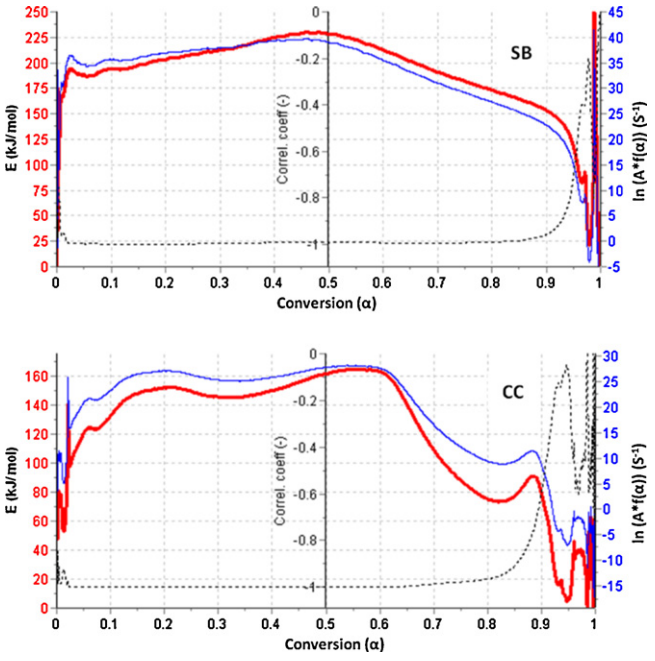

Fig. 2. Apparent E, $\ln(A{\cdot}f(\alpha))$ dependence on conversion for CC and SB with E (——), $\ln(A{\cdot}f(\alpha))$ (——) and the calculated correlation coefficients (.....).

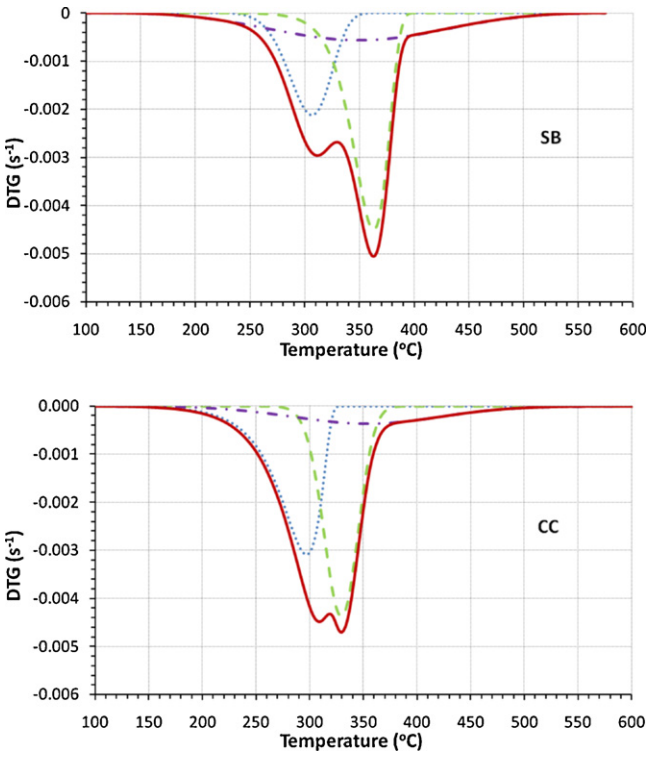

Fig. 3. Deconvolution of DTG curves for CC and SB at 20 °C min^{-1} with hemicelluloses (•••), cellulose (— —), lignin (— • —) and the sum of the curves (——).

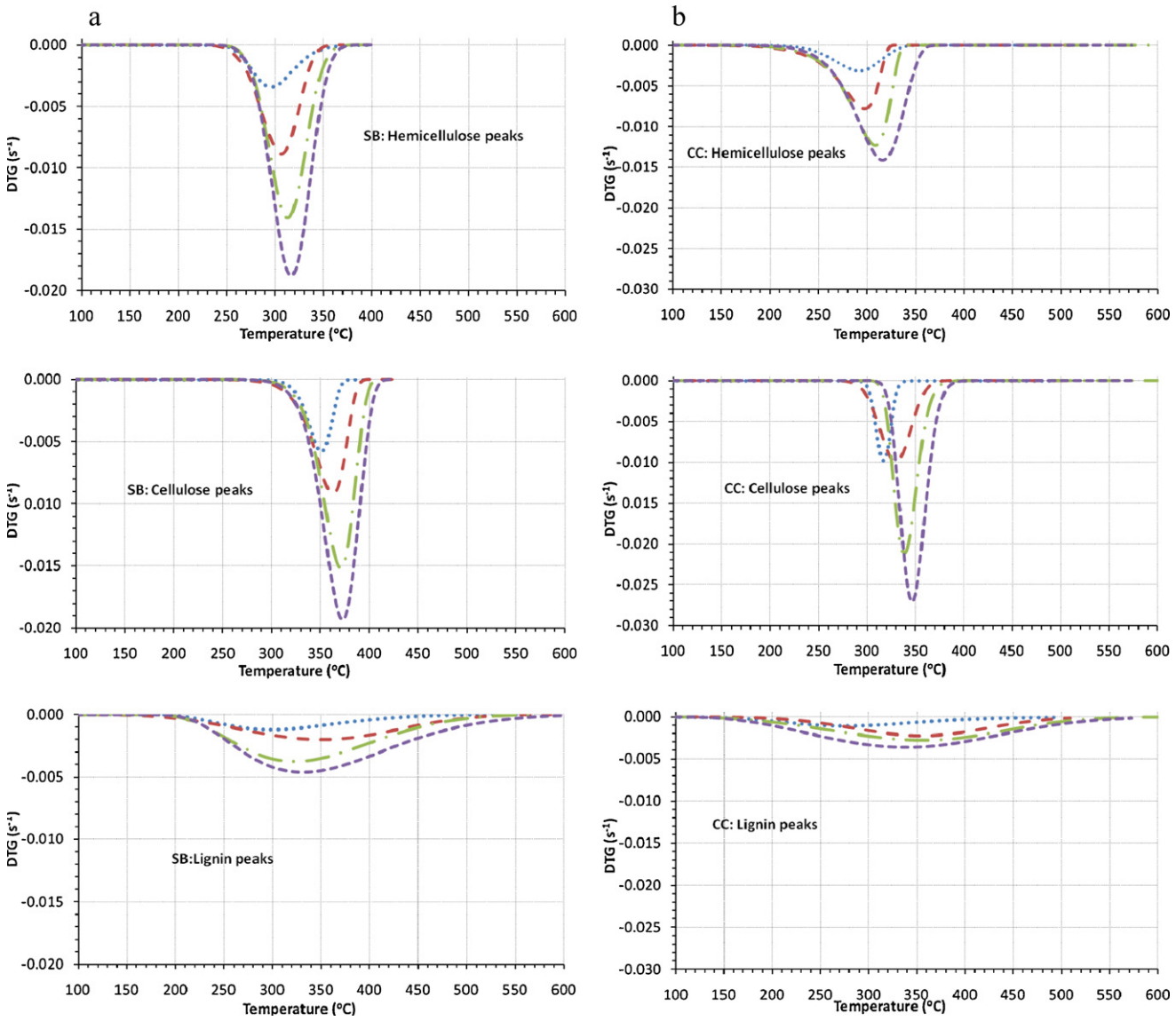

Fig. 4. DTG of SB and CC pseudocomponents obtained by deconvolution of global curves with 10 °C min^{-1} ( ), 20 °C min^{-1} ( ), 30 °C min^{-1} ( ) and 40 °C min^{-1} ( ).

ature and extent of reaction [2], and frequently overlap one another. This factor limits the theoretical utility of such global kinetic parameters in describing specific decomposition reactions mechanisms since no particular reactions can be identified [2,40]. Nevertheless some general tendencies in the global reaction mechanism can still be drawn. For instance, the results could allow a qualitative comparison of the reactivity of both fuels, since higher apparent E values are generally due to the decomposition of the less reactive components in biomass [6]. Based on this, it can be deduced that CC is more reactive than SB. The catalytic effect of ash was not readily discernable, since the higher ash content in SB should result in lower activation energy, which was not observed. This suggests that factors other than ash are more prominent. The overall trend of $E(\alpha)$ for SB and CC in Fig. 2 also indicates that the less reactive constituents decompose at earlier stages of conversion followed in the later stages ($\alpha > 0.6$) by the more reactive components corresponding to lower E values. The decreasing trend of $E(\alpha)$ at higher conversion agrees with reported results from some previous studies [11] based on similar biomass materials but contradicts a few others [6,8]. This again highlights the unreliability of the theoretical

Table 4
Quality of fit (QOF) values obtained from comparing simulated and experimental DTG curves using both global and pseudocomponent analysis.

Heating rate (°C min^{-1})	Global analysis (QOF of DTG curves, %)		Pseudocomponent analysis (QOF of DTG curves, %)	
	CC	SB	CC	SB
10	2.1	1.9	6.8	1.8
20	3.8	1.4	6.7	1.7
30	2.1	1.7	3.3	3.1
40	1.8	0.5	2.9	1.9
50	6.9	2.3	9.6	5.3

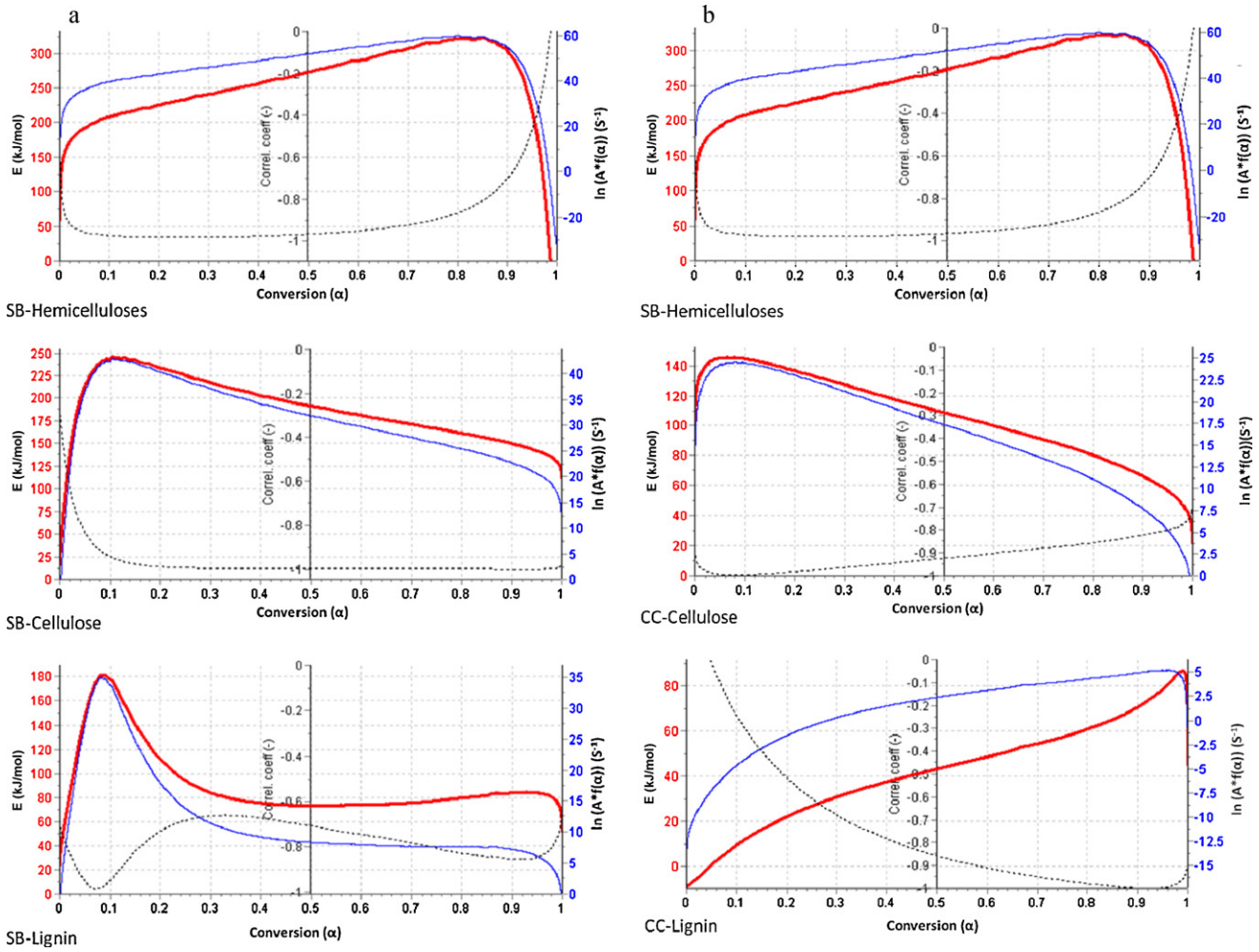

Fig. 5. Apparent E and $\ln(A{\cdot}f(\alpha))$ dependences on conversion for the pseudocomponents with E (▬), $\ln(A{\cdot}f(\alpha))$ (▬) and the calculated correlation coefficients (┅).

or mechanistic interpretation of the kinetic trends obtained from complex materials.

3.3. Kinetic analysis of pseudocomponents

It is widely recognised that the devolatilization behaviour of lignocellulosic biomass is heavily dependent on the behaviour of their constituent components namely hemicelluloses, cellulose and lignin [24,40,41]. Considering that similar experimental conditions (i.e. heating rate, temperature, pressure and particle size) were employed, the difference in the devolatilization and apparent kinetic trends between the two fuels can be attributed to the differences between the relative composition and nature of these components. Analysis of pseudocomponents representing these constituents was accomplished by first deconvoluting the DTG curves of the samples as described in the methodology section. The results of the deconvolution are displayed in Fig. 3 and the derived percentage contribution of the separated peaks to the total curve area is provided in Table 3. The percentage contribution of the pseudocomponents shown in Table 3 are broadly in the range of chemical composition values reported in literature for SB; 20–32% hemicelluloses, 31–40% cellulose, 18–27% lignin, and 6–25% extractives [42–45]. For CC, reported values range between 32% and 40.6% for SB hemicelluloses, 34–51% for cellulose, 3–19% for lignin, and 4.9–12.6% for extractives [30,46–49] differ significantly from our results particularly with reference to lignin which seems to be overestimated at the expense of cellulose. Deviations from the reported values for both samples could be explained by the presence of alcohol–benzene–water-soluble extractives which could represent up to 25 wt.% of the original untreated material [42]. The devolatilization of extractives generally occurs in the same range of temperature as hemicelluloses and parts of lignin. This effect also highlights why the deconvoluted peaks cannot, strictly speaking, be assigned to specific components. Hence the use of the term 'pseudocomponents' in literature [1], where reaction steps represented by the peaks are thought to be dominated by one component or the other. For these peaks to be realistically considered as true representations of lignocellulosic components, a calibration using TGA results of each of the extracted components may be necessary in the manner shown by Carrier et al. [50].

The high deviation within the reported composition values themselves partly point to the heterogeneous nature of biomass, but may also be attributed to the different methodologies employed in determining composition. Whereas the chemical composition of cellulose is known to vary little between biomass materials, the types and properties of hemicelluloses and lignin often differ widely [41], further highlighting the heterogeneous nature of various lignocellulosic biomasses. In addition, the amount and composition of ash contained within biomass are known to influence devolatilization, as mentioned earlier. All of the aforementioned is reflected in the variance observed in Table 1 between proximate

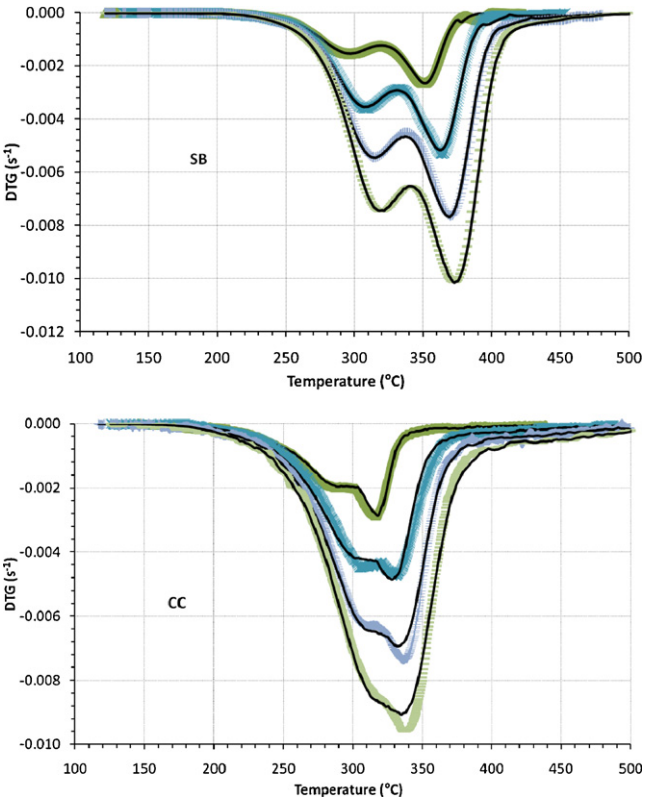

Fig. 6. Reproduction of experimental DTG curves for heating rates 10–40 °C min^{-1} based on parameters from global kinetic analysis with 10 °C min^{-1} (▲), 20 °C min^{-1} (X), 30 °C min^{-1} (+), 40 °C min^{-1} (▬) and simulated curves (▬).

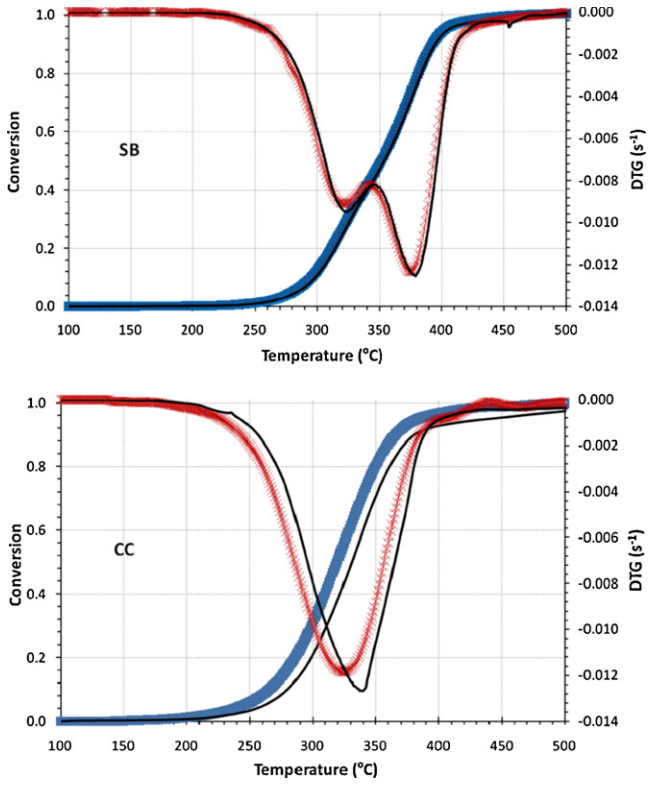

Fig. 7. Comparison of experimental and predicted DTG curves for 50 °C min^{-1} heating rate based on parameters from global kinetic analysis with TG-experimental (▬), DTG-experimental (X) and predicted curves (▬).

and ultimate parameters derived for this study and those from previous authors.

To obtain the kinetics of each pseudocomponent, peaks representing them were extracted from each heating rate and are shown grouped together in Fig. 4. From these peaks, apparent E and $\ln(A{\cdot}f(\alpha))$ dependence on α for each pseudocomponent were derived via the same isoconversional analysis employed for global single component analysis and are shown in Fig. 5. The $E(\alpha)$ trends for both materials confirm that the decomposition of the pseudocomponents also proceeds via a multi-step process comprising numerous complex reactions.

The concerns mentioned during the discussion of global kinetic analysis above, about the apparent nature of E, apply even more to pseudocomponents analysis because of the extra mathematical manipulations involved. Therefore even more care must be taken in deriving theoretical interpretations from the results, especially when the poor correlation coefficients shown in Fig. 5 are also considered. In general, it can be observed that the apparent E obtained for each pseudocomponent is largely consistent with literature where often lower activation energy values are reported for lignin (18–65 kJ mol^{-1}) than for cellulose (195–286 kJ mol^{-1}) or hemicelluloses (80–116 kJ mol^{-1}) [24,25]. The fact that these reported values were obtained via a different analytical approach (model-fitting) gives an indication of the reliability of our approach. Another indicator of our method's versatility can be obtained by validating simulations produced from the results with experimental data as shown in the next section.

3.4. Validation of kinetic analysis approach

Ultimately, the main usefulness of kinetic analysis of polymers such as biomass is more practical than theoretical. According to Vyazovkin [3] and Varhegyi [1], kinetic analysis should also include

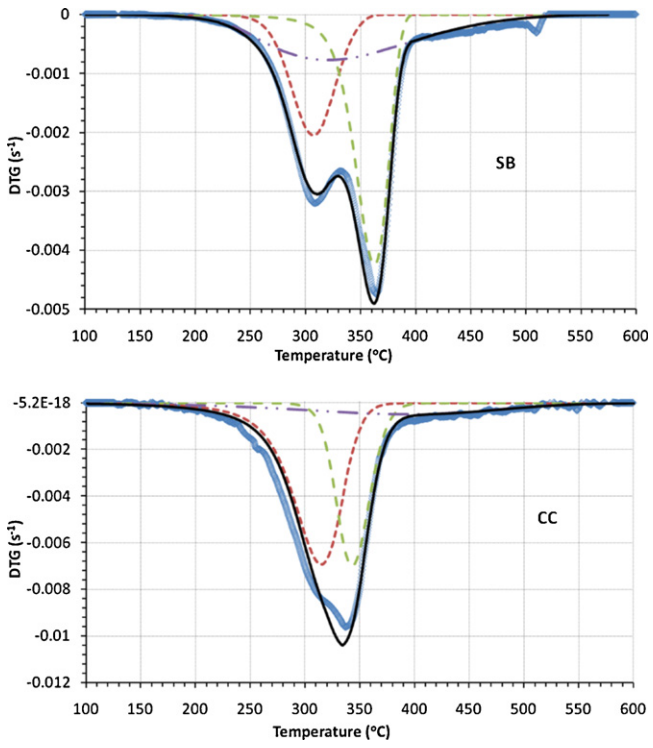

Fig. 8. Reproduction of experimental curves for SB (20 °C min^{-1}) and CC (40 °C min^{-1}) based on kinetic analysis of pseudocomponents with hemicelluloses (▬), cellulose (▬) and lignin (▬), total predicted (▬) and experimental curves (O).

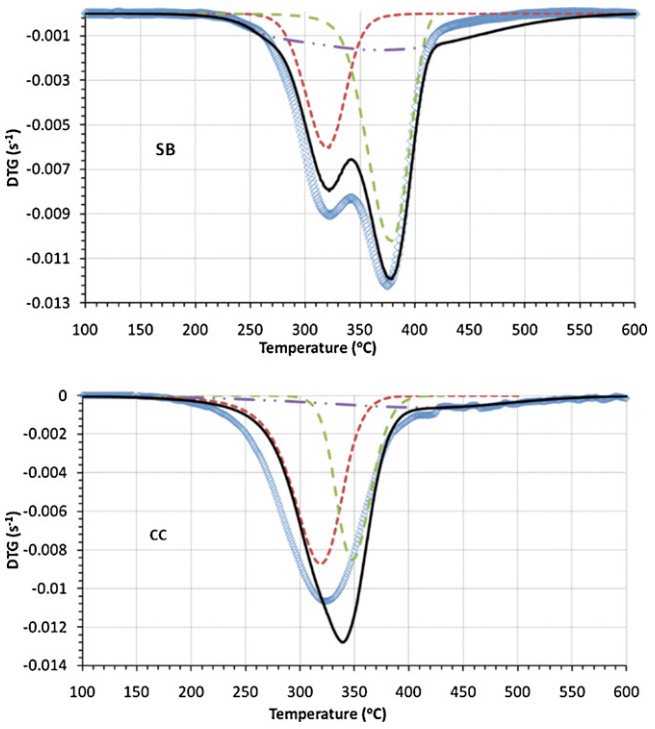

Fig. 9. Comparison of predicted and experimental curves for SB and CC at 50 °C min^{-1} heating rate based on kinetic analysis of pseudocomponents with hemicelluloses ( ), cellulose ( ), lignin ( ), total predicted ( ) and experimental curves ( ).

the practical ability to simulate and predict degradation rates which help in the design and sizing of thermochemical process reactors. For the current paper, the validation was achieved by simulating the heating rate curves employed in the analysis, and by predicting the reaction rate progress at a different heating rate, 50 °C min^{-1}, not used in the analysis.

In traditional kinetic analysis, it is normally expected that all three parameters that form the kinetic triplets – activation energy (E), pre-exponential factors (A) and decomposition function ($f(\alpha)$) – are needed in order to predict TG or DTG curves using Eq. (1). However, Vyazovkin [4] showed that it was not necessary to derive these parameters when isoconversional analysis is applied. In the first place their theoretical relevance as a tool for interpreting reaction mechanism has been questioned [2]. Furthermore their practical relevance in terms of simulating or predicting reaction progress or reaction rate data are rendered redundant (during isoconversional analysis) as reaction curve predictions can be readily obtained from Eq. (4). Fig. 6 shows a reproduction of the DTG curves (10, 20, 30 and 40 °C min^{-1}) used in the kinetic analysis from the results obtained from global kinetic analysis. The quality ranging of fits obtained using Eq. (5) between the simulated and experimental DTG curves for both CC and SB are shown in Table 4. The fit values displayed in Table 4 using the global, single component analytical approach compared well with those obtained via conventional model fitting approaches employed in previous reports. Branca et al. [24] who employed multi-heating rate, multi-component model fitting on wood devolatilization obtained fits from 3% to 26% using a 1, 2, and 3 independent parallel reactions model. Gronli et al. [25] obtained better fits ranging from 0.6% to 2.2% using a 5 parallel reactions model. This clearly shows that model-free methods produce comparably reliable predictions to multiple heating rate model-fitting methods.

Another indication of the reliability of the kinetic analysis method is the ability to predict reaction progress for heating rates outside the range used in the analysis. Fig. 7 shows good agreement between the predicted and experimental TG and DTG curves for CC and SB at 50 °C min^{-1}. The fit values obtained are comparable to those obtained at heating rates within the range used for kinetic analysis.

Simulation and prediction from pseudocomponent analysis were achieved using Eqs. (3) and (4). First, Eq. (4) was applied to each pseudocomponent, and then the global curve was calculated as the weighted sum of the simulated curves assigned to the pseudocomponents according to Eq. (3). Fig. 8 shows the reproduction of curves employed in the analysis while Fig. 9 shows the predicted reaction rate at 50 °C min^{-1}. In both cases, simulated or predicted curves were compared with experimental data and the QOFs obtained are presented in Table 4. The results show a better fit between simulated and experimental curves for SB than for CC. Compared to results from the global kinetic approach, generally lower fits were obtained from the analysis of pseudocomponents, probably as a results of errors from mathematical manipulations of the data during the deconvolution. However, fits obtained from the pseudocomponent analysis are still comparable and in some cases better than those derived from conventional model-fitting as mentioned above.

4. Conclusions

The thermokinetics of the devolatilization of two of the most prominent agricultural residues in South Africa, corn cobs and sugar cane bagasse, have been investigated in this paper by thermogravimetric analysis. Friedman's isoconversional analysis was applied to global and deconvoluted DTG curves to obtain the dependence of the kinetic parameters on conversion for the samples and their constituent pseudocomponents.

To our knowledge, this study represents the only attempt to use this approach. Some differences in the devolatilization characteristics (devolatilization rates, peak temperatures and kinetics parameters) were observed between the two fuels and their pseudocomponents, with sugar cane bagasse having generally higher activation energy values than corn cobs. Considering that similar experimental conditions (i.e. heating rate, temperature, pressure and particle size) were employed, this could be attributed to the differences between the relative composition and nature of these components. However, these observed differences between the two agricultural wastes studied where relatively small, and may suggest that there are no kinetic barriers to the thermal co-processing of these fuels, where other factors such as heat and transport phenomena are not limiting.

Furthermore, it was pointed out that while some useful theoretical interpretations of the kinetic parameters are possible, the main utility of these kinetic parameters is their applicability to the prediction of experimental decomposition data. Results from both global and pseudocomponent analysis were therefore used to simulate experimental curves and reasonably high fits between simulated and experimental data were obtained, comparable to those obtained from model-fitting studies. This implies that the results can be reliably used in the design and optimization of the devolatilization section of reactors used in thermochemical processes where low heating rates occur, such as slow pyrolysis/carbonisation and updraft fixed bed gasification.

Acknowledgements

This research was conducted in part with funds from the South African National Research Foundation, the South African National Energy Research Institute, Fort Hare Institute of Technology (South Africa), and Karlsruhe Institute of Technology's (Germany) basic funding.

References

[1] G. Varhegyi, Aims and methods in non-isothermal reaction kinetics, Journal of Analytical and Applied Pyrolysis 79 (2007) 278–288.
[2] S. Vyazovkin, Model-free kinetics, Journal of Thermal Analysis and Calorimetry 83 (2006) 45–51.
[3] S. Vyazovkin, Computational aspects of kinetic analysis Part C: the ICTAC Kinetics Project – the light at the end of the tunnel? Thermochimica Acta 355 (2000) 155–163.
[4] S. Vyazovkin, A unified approach to kinetic processing of nonisothermal data, International Journal of Chemical Kinetics 28 (1996) 95–101.
[5] M. Garcià-Pèrez, A. Chaala, J. Yang, C. Roy, Co-pyrolysis of sugarcane bagasse with petroleum residue. Part I: thermogravimetric analysis, Fuel 80 (2001) 1245–1258.
[6] E. Biagini, A. Fantei, L. Tognotti, Effect of the heating rate on the devolatilization of biomass residues, Thermochimica Acta 472 (2008) 55–63.
[7] E. Biagini, L. Guerrini, C. Nicolella, Development of a variable energy model for biomass 361 devolatilization, in: Chemical Engineering Transactions, 2009, pp. 1–6.
[8] J.M. Cai, L.S. Bi, Kinetic analysis of wheat straw pyrolysis using isoconversional methods, Journal of Thermal Analysis and Calorimetry 98 (2009) 325–330.
[9] J. Cai, S. Chen, R. Liu, Weibull mixture model for isoconversional kinetic analysis of biomass oxidative pyrolysis, Journal of the Energy Institute 82 (2009) 238–241.
[10] J. Cai, R. Liu, C. Sun, Logistic regression model for isoconversional kinetic analysis of cellulose pyrolysis, Energy & Fuels 22 (2008) 867–870.
[11] V. Leroy, D. Cancellieri, E. Leoni, J. Rossi, Kinetic study of forest fuels by TGA: model-free kinetic approach for the prediction of phenomena, Thermochimica Acta 497 (2010) 1–6.
[12] L. Gašparovič, Z. Koreňová, Ľ. Jelemenský, Kinetic study of wood chips decomposition by TGA, Chemical Papers 64 (2009) 174–181.
[13] H. Xiao, X. Ma, Z. Lai, Isoconversional kinetic analysis of co-combustion of sewage sludge with straw and coal, Applied Energy 86 (2009) 1741–1745.
[14] Y. Tonbul, Pyrolysis of pistachio shell as a biomass, Journal of Thermal Analysis and Calorimetry 91 (2007) 641–647.
[15] A.G. Santos, A.S. Araujo, V.P. Caldeira, V.J. Fernandes Jr., L.D. Souza, A.K. Barros, Model-free kinetics applied to volatilization of Brazilian sunflower oil, and its respective biodiesel, Thermochimica Acta 506 (2010) 57–61.
[16] L Lynd, H. Von Blottnitz, B. Tait, J. de Boer, I. Pretorius, K. Rumbold, et al., Converting plant biomass to fuels and commodity chemicals in South Africa: a third chapter? South African Journal of Science 99 (2003) 499–507.
[17] Department of Minerals and Energy, White Paper on the Renewable Energy Policy of the Republic of South Africa, Department of Minerals and Energy, 2003.
[18] M.J. Antal, G. Varhegyi, Cellulose pyrolysis kinetics: the current state of knowledge, Industrial & Engineering Chemistry Research 34 (1995) 703–717.
[19] C. Di Blasi, G. Signorelli, C. Di Russo, G. Rea, Product distribution from pyrolysis of wood and agricultural residues, Industrial & Engineering Chemistry Research 38 (1999) 2216–2224.
[20] C. Di Blasi, G. Signorelli, G. Portoricco, Countercurrent fixed-bed gasification of biomass at laboratory scale, Industrial & Engineering Chemistry Research 38 (1999) 2571–2581.
[21] M.E. Brown, Introduction to Thermal Analysis: Techniques and Applications, Kluwer Academic Publishers, 2001.
[22] H.L. Friedman, Kinetics of Thermal Degradation of Char-Forming Plastics from Thermogravimetry. Application to a Phenolic Plastic, Wiley Subscription Services, Inc., A Wiley Company New York, 1964.
[23] G. Varhegyi, M.J. Antal, T. Szekely, P. Szabo, Kinetics of the thermal decomposition of cellulose, hemicellulose, and sugarcane bagasse, Energy & Fuels 3 (1989) 329–335.
[24] C. Branca, A. Albano, C. Di Blasi, Critical evaluation of global mechanisms of wood devolatilization, Thermochimica Acta 429 (2005) 133–141.
[25] M.G. Gronli, G. Varhegyi, C. Di Blasi, Thermogravimetric analysis and devolatilization kinetics of wood, Industrial & Engineering Chemistry Research 41 (2002) 4201–4208.
[26] J.A. Caballero, J.A. Conesa, Mathematical considerations for nonisothermal kinetics in thermal decomposition, Journal of Analytical and Applied Pyrolysis 73 (2005) 85–100.
[27] AKTS, AKTS Advanced Thermal Analysis Software, http://www.akts.com/ (2010).
[28] A. Iliyas, K. Hawboldt, F. Khan, Advanced kinetics for calorimetric techniques and thermal stability screening of sulfide minerals, Thermochimica Acta 501 (2010) 35–45.
[29] P. Roque-Diaz, C. University, L.C.V. Villas, Zh. Shemet, V.A. Lavrenko, V.A. Khristich, Studies on thermal decomposition and combustion mechanism of bagasse under non-isothermal conditions, Thermochimica Acta 93 (1985) 349–352.
[30] O. Ioannidou, A. Zabaniotou, E.V. Antonakou, K.M. Papazisi, A.A. Lappas, C. Athanassiou, Investigating the potential for energy fuel materials and chemicals production from corn residues (cobs and stalks) by non-catalytic and catalytic pyrolysis in two reactor configurations, Renewable and Sustainable Energy Reviews 13 (2009) 750–762.
[31] A. Kumar, L. Wang, Y.A. Dzenis, D.D. Jones, M.A. Hanna, Thermogravimetric characterization of corn stover as gasification and pyrolysis feedstock, Biomass and Bioenergy 32 (2008) 460–467.
[32] K.G. Mansaray, A.E. Ghaly, Determination of kinetic parameters of rice husks in oxygen using thermogravimetric analysis, Biomass and Bioenergy 17 (1999) 19–31.
[33] F. Shafizadeh, Introduction to pyrolysis of biomass, Journal of Analytical and Applied Pyrolysis 3 (1982) 283–305.
[34] E. Biagini, F. Barontini, L. Tognotti, Devolatilization of biomass fuels and biomass components studied by TG/FTIR technique, Industrial & Engineering Chemistry Research 45 (2006) 4486–4493.
[35] P. Luangkiattikhun, C. Tangsathitkulchai, M. Tangsathitkulchai, Non-isothermal thermogravimetric analysis of oil-palm solid wastes, Bioresource Technology 99 (2008) 986–997.
[36] H. Haykiri-Acma, S. Yaman, S. Kucukbayrak, Effect of heating rate on the pyrolysis yeilds of rapeseed, Renewable Energy 31 (2006) 803–810.
[37] C. Di Blasi, Modeling chemical and physical processes of wood and biomass pyrolysis, Progress in Energy and Combustion Science 34 (2008) 47–90.
[38] Q. Cao, K. Xie, W. Bao, S. Shen, Pyrolytic behaviour of waste corn cob, Bioresource Technology 94 (2004) 83–89.
[39] A. Zabaniotou, O. Ioannidou, E. Antonakou, A.A. Lappas, Experimental study of pyrolysis for potential energy, hydrogen and carbon material production from lignocellulosic biomass, International Journal of Hydrogen Energy 33 (2008) 2433–2444.
[40] B.A. Howell, Utility of kinetic analysis in the determination of reaction mechanism, Journal of Thermal Analysis and Calorimetry 85 (2006) 165–167.
[41] F. Shafizadeh, Introduction to pyrolysis of biomass, Journal of Analytical and Applied Pyrolysis (1982).
[42] P. Das, A. Ganesh, P. Wangikar, Influence of pretreatment for deashing of sugarcane bagasse on pyrolysis products, Biomass and Bioenergy 27 (2004) 445–457.
[43] A.F. Drummond, I.W. Drummond, Pyrolysis of sugar cane bagasse in a wire-mesh reactor, Industrial & Engineering Chemistry Research 35 (1996) 1263–1268.
[44] E.S. Lipinsky, Perspectives on preparation of cellulose for hydrolysis, in: Hydrolysis of Cellulose: Mechanisms of Enzymatic and Acid Catalysis, American Chemical Society, 1979, 1–23.
[45] S. Munir, S. Daood, W. Nimmo, A. Cunliffe, B. Gibbs, Thermal analysis and devolatilization kinetics of cotton stalk, sugar cane bagasse and shea meal under nitrogen and air atmospheres, Bioresource Technology 100 (2009) 1413–1418.
[46] C.A. Koufopanos, A. Lucchesi, G. Maschio, Kinetic modelling of the pyrolysis of biomass and biomass components, The Canadian Journal of Chemical Engineering 67 (1989) 75–84.
[47] B. Rivas, A.B. Moldes, J.M. Domínguez, J.C. Parajó, Lactic acid production from corn cobs by simultaneous saccharification and fermentation: a mathematical interpretation, Enzyme and Microbial Technology 34 (2004) 627–634.
[48] N. Pece, N. Perotti, O. Molina, Bacterial protein production from corn cob pretreated with NaOH at room temperature, World Journal of Microbiology and Biotechnology 10 (1994) 593–594.
[49] T. Sonobe, N. Worasuwannarak, S. Pipatmanomai, Synergies in co-pyrolysis of Thai lignite and corncob, Fuel Processing Technology 89 (2008) 1371–1378.
[50] M. Carrier, A. Loppinet-Serani, D. Denux, J. Lasnier, F. Ham-Pichavant, F. Cansell, et al., Thermogravimetric analysis as a new method to determine the lignocellulosic composition of biomass, Biomass and Bioenergy 35 (2011) 298–307.